Compartment-dependent activities of Wnt3a/β-catenin signaling during vertebrate axial extension

Arnon Dias Jurberg[1*], Rita Aires[1], Ana Nóvoa[1], Jennifer Elizabeth Rowland[1] and Moisés Mallo[1,#]

1 Instituto Gulbenkian de Ciência. Rua da Quinta Grande 6. 2780-156 Oeiras. Portugal

* Present address: Laboratory on Thymus Research, Oswaldo Cruz Institute, Oswaldo Cruz Foundation/Fiocruz, Av. Brasil, 4365. Pavilhão Leônidas Deane, Manguinhos, Rio de Janeiro, RJ, Brazil. 21040-360 and Graduate Program in Cell and Developmental Biology, Institute of Biomedical Sciences (ICB), Federal University of Rio de Janeiro, Rio de Janeiro, RJ, Brazil. 21941-902.

Key words: Wnt signaling, axial progenitors, patterning, mouse development

Running title: Wnt3a during axial extension

#Correspondence to M. Mallo
Tel: +351-214464624
Fax: +351-214407970
e-mail: mallo@igc.gulbenkian.pt

Abstract

Extension of the vertebrate body results from the concerted activity of many signals in the posterior embryonic end. Among them, Wnt3a has been shown to play relevant roles in the regulation of axial progenitor activity, mesoderm formation and somitogenesis. However, its impact on axial growth remains to be fully understood. Using a transgenic approach in the mouse, we found that the effect of Wnt3a signaling varies depending on the target tissue. High levels of *Wnt3a* in the epiblast prevented formation of neural tissues, but did not impair axial progenitors from producing different mesodermal lineages. These mesodermal tissues maintained a remarkable degree of organization, even within a severely malformed embryo. However, from the cells that failed to take a neural fate, only those that left the epithelial layer of the epiblast activated a mesodermal program. The remaining tissue accumulated as a folded epithelium that kept some epiblast-like characteristics. Together with previously published observations, our results suggest a dose-dependent role for Wnt3a in regulating the balance between renewal and selection of differentiation fates of axial progenitors in the epiblast. In the paraxial mesoderm, appropriate regulation of Wnt/β-catenin signaling was required not only for somitogenesis, but also for providing proper anterior-posterior polarity to the somites. Both processes seem to rely on mechanisms with different requirements for feedback modulation of Wnt/β-catenin signaling, once segmentation occurred in the presence of high levels of Wnt3a in the presomitic mesoderm, but not after permanent expression of a constitutively active form of β-catenin. Together, our findings suggest that Wnt3a/β-catenin signaling plays sequential roles during posterior extension, which are strongly dependent on the target tissue. This provides an additional example of how much the functional output of signaling systems depends on the competence of the responding cells.

Introduction

Formation of the vertebrate body requires a combination of well coordinated cell proliferation and differentiation processes. After initial patterning events that define the embryonic anterior-posterior (AP) axis and trigger gastrulation, most of the embryo is made by sequential addition of new tissue at its posterior end (Stern et al., 2006). These tissues are continuously produced from axial progenitors that have been suggested to have stem cell-like properties (Wilson et al., 2009). In a first phase, these progenitors are localized in the epiblast and respond to the organizing activity of the primitive streak (PS). Later in development, axial progenitors relocate to the tail bud, which becomes the driver for posterior growth (Wilson et al., 2009). These progenitors comprise a heterogeneous population, which include a group of bipotent neuro-mesodermal (N-M) cells able to originate both neural tube and paraxial mesoderm all along the AP body axis (Wilson et al., 2009; Tzouanacou et al., 2009). N-M progenitors are first located in the region between the node and the anterior part of the PS, known as the node-streak border, and later in the chordo-neural hinge within the tail bud (Cambray and Wilson, 2002; 2007; Tzouanacou et al., 2009). In addition to the N-M progenitors, the epiblast also contains progenitor cells for the lateral and intermediate mesoderm, which in association with the endoderm assemble most of the trunk-related organs (Carlson, 1999).

Recent findings suggest that Wnt3a signaling is a major determinant of bipotent N-M progenitor fates. It has been reported that Wnt3a, in conjunction with Fgf signaling, controls *Sox2* expression in the anterior epiblast, suggesting a role for Wnt signaling in the production of neural tissues (Takemoto et al., 2006; 2011). In addition, functional analyses both in zebrafish and in mouse embryos indicate that *Wnt3a* plays an essential role in the production of paraxial mesoderm from these progenitors. In the zebrafish embryo, N-M cells take a neural or mesodermal fate depending on whether the Wnt3a/β-catenin pathway is blocked or stimulated, respectively (Martin and Kimelman, 2012). Likewise, *Wnt3a* mutant mouse embryos are truncated posterior to the forelimbs, with strong reduction of mesodermal structures and over-production of neural tissues

(Takada et al., 1994; Yoshikawa et al., 1997), indicating that *Wnt3a* is required for both maintenance of the progenitor pool and production of mesodermal fates. However, *Wnt3a* is down regulated when the N-M progenitor derivatives enter the mesodermal compartment by a *Tbx6*-dependent mechanism (Takemoto et al., 2011). This down regulation seems to be required for somitogenesis as sustained activation of β-catenin in the PSM resulted in an enlarged PSM and in a strong inhibition of segmentation posterior to the first few somites (Aulehla et al., 2008; Dunty et al., 2008). Interestingly, it has been suggested that the presence of ectopic neural tubes, replacing the paraxial mesoderm of *Tbx6* mutant embryos, is derived from persistent *Wnt3a* expression in this tissue (Takemoto et al., 2011). This idea seems to be at odds with the incompatibility between Wnt3a/β-catenin signaling and neural differentiation of bipotent progenitors described in zebrafish embryos (Martin and Kimelman, 2012) and raises the possibility that the biological effects of Wnt3a/β-catenin signaling during vertebrate axial growth depend on the tissue context.

Here, we show that activation of *Wnt3a* or *β-catenin* in different embryonic compartments produces dissimilar effects during early patterning and growth processes in the mouse embryo. Over-expression of *Wnt3a* in the epiblast prior to cell ingression through the PS resulted in shorter embryos with strong malformations posterior to the forelimb buds. Molecular analyses indicate that elevated *Wnt3a* expression in the epiblast impaired neural development, while still allowing mesodermal differentiation with a considerable degree of AP patterning. However, from the cells that failed to take a neural fate, only those that left the epithelial layer of the epiblast activated a mesodermal program. This generated a folded epithelium that preserved some characteristics normally observed in the epiblast. Conversely, over-expression of *Wnt3a* or stabilizing β-catenin in the PSM promoted mesodermal fates with no apparent impact on neural differentiation. Interestingly, contrary to stabilized β-catenin activity, sustained *Wnt3a* expression in the PSM allowed somite formation but these somites had altered AP polarity, thus revealing an additional role for *Wnt3a* in somitogenesis. Altogether, our findings uncover dissimilar effects of *Wnt3a*

activity in the axial progenitors and its derived mesodermal tissues, providing an additional example of differential responses triggered by the same signaling molecule during vertebrate development.

Materials and Methods

Generation and analysis of transgenic embryos

Transgenic constructs were generated by cloning the *Wnt3a* cDNA downstream of the 9.5 kb fragment enhancer of the *Cdx2* gene (Benahmed et al., 2008) or the *msd* enhancer of *Dll1* (Beckers et al., 2000), using standard molecular biology techniques. Constructs were released from plasmid sequences, gel purified and used to generate transgenic embryos by pronuclear microinjection. *T-Cre::β-catenin*$^{del(ex3)/+}$ embryos were generated as previously described (Aulehla et al., 2008), using the *T-Cre* (Perantoni et al., 2008) and *Catnb*$^{lox(ex3)/+}$ (Harada et al., 1999) mouse strains. *Cdx2P-Cre*^{ERT}*;;ROSA26-R* embryos have been previously described (Jurberg et al., 2013). *T-Cre*^{ERT}*;;ROSA26-R* embryos were produced by crossing the ROSA26-R mice (Soriano, 1999) with a transgenic line expressing *Cre*^{ERT} (Hayashi and McMahon, 2002) under the *T* enhancer. All experiments conducted on animals followed the Portuguese (Portaria 1005/92) and European (Directive 2010/63/EU) legislations, concerning housing, husbandry, and welfare. The project was reviewed and approved by the Ethics Committee of ‘‘Instituto Gulbenkian de Ciência’’ and by the Portuguese National Entity, ‘‘Direcção Geral de Alimentação e Veterinária’’ (license reference: 014308).

Embryos were collected by cesarean section, fixed in 4% PFA and analyzed by whole mount in situ hybridization as previously described (Kanzler et al., 1998) or fixed in Mirsky's fixative and stained for β-galactosidase activity as described elsewhere (Carvajal et al. 2001). Morphological examination using carmine staining was performed as previously described (Jurberg et al., 2013). For whole-mount PECAM-1 immunostaining, PFA-fixed embryos were washed in PBS, dehydrated and rehydrated in methanol/PBT (PBS containing 0.1% Tween

20) series, and washed twice in PBT. Embryos were blocked overnight in PBS containing 1% BSA and 0.5% Tween-20 at 4º C, under agitation. They were then washed three times in PBT and incubated overnight in the primary antibody solution (1/100 PECAM-1/CD31 diluted in 0.5% BSA, 0.25% Tween-20 in PBS) at 4º C, under agitation. Embryos were then washed thoroughly in PBT at room temperature and incubated overnight in the secondary antibody solution (1/100 goat anti-rat Alexa488 diluted in 0.5% BSA, 0.25% Tween-20 in PBS) at 4º C, under agitation and protected from light. They were washed thoroughly in PBT at room temperature, in the dark, and dehydrated in a methanol/PBT series. Then, embryos were cleared in a methyl salicylate/methanol series and imaged by laser scanning confocal microscopy (Zeiss LSM-510 Meta).

Results

Stabilization of β-catenin in mesodermal tissues results in impaired somitogenesis with no apparent impact on neural fate

The role of Wnt/β-catenin in somitogenesis has been evaluated by inducing stable expression in mesodermal tissues of a constitutive active form of β-catenin (*β-catenin*$^{del(ex3)}$) from the ROSA26 locus, by means of Cre recombinase expressed under the control of an enhancer of the *T(Brachyury)* gene (*T-Cre::β-catenin*$^{del(ex3)/+}$ embryos, Aulehla et al., 2008). These embryos have an expanded PSM with a virtual absence of somitogenesis after the first few somites. To evaluate the fate of the PSM tissue that failed to produce somites, we let these embryos develop until embryonic stage (E)10.5. At this stage, *T-Cre::β-catenin*$^{del(ex3)/+}$ embryos presented malformations that correlated with those observed in younger embryos (Aulehla et al., 2008). These included the absence of most of the normal embryonic structures posterior to the heart region, which were replaced to a large extent by an amorphous tissue mass ventral to a kinked structure with neural tube characteristics (Fig. 1). Molecular analyses indicated that this ventral mass was positive for *Tbx6*, with no traces of *Sox2* expression

(Fig. 1A-D). This revealed that sustained β-catenin activation in the PSM did not promote neural differentiation, but rather it led to a continuous accumulation of non-segmented paraxial mesoderm. Although *Sox2* expression was absent from the amorphous tissue mass, it was very strong in the twisted dorsal structure extending along the whole AP embryonic axis of *T-Cre::β-catenin*$^{del(ex3)/+}$ embryos (Figs 1B and S2B,B'), thus confirming the neural identity of this structure. It is possible that the kinked morphology of the neural tube derived from a normal growing structure fitting to a shorter AP body length imposed by the abnormal development of the mesodermal compartments in these embryos.

In addition to the neural tube, *T-Cre::β-catenin*$^{del(ex3)/+}$ embryos presented other characteristics indicative of an unexpected degree of conservation of normal embryonic patterns. They had a recognizable tail bud (Figs 1 and S2B), which displayed some structural characteristics similar to those observed in wild type embryos, such as a dorso-medial *Sox2*-positive neural tube (Fig. S2A,A',B,B') and a *Tbx6*-positive PSM (Fig. 1C,D), which remained unable to form somites. We also observed signs of some AP pattern conservation in those embryos. In particular, *Hoxc10* presented a clear anterior expression border both in the neural tube and in the *Tbx6*-positive mass (Fig. 1E,F). Although *T-Cre::β-catenin*$^{del(ex3)/+}$ embryos lacked mesodermal landmarks normally used to estimate the AP level of this expression border, such as somites and hindlimb buds, its anterior expression boundary in the neural tube did not seem to be anteriorized when compared with wild type embryos (Fig. 1E,F). The coincidence of the *Hoxc10* anterior expression limits in neural and mesodermal tissues of the mutant embryos also suggests that this gene is not further stimulated by β-catenin in the mesoderm. In addition, we could detect some *Tbx4*-positive spots in the posterior region of *T-Cre::β-catenin*$^{del(ex3)/+}$ embryos, including a ventro-medial domain located between the posterior border of the enlarged *Tbx6*-positive mass and the antero-ventral border of the tail bud (Fig. 1H). This pattern of *Tbx4* expression is consistent with the presence of ventral lateral mesoderm, typically associated with the trunk to tail transition (Fig. 1G). Other more lateral *Tbx4*-positive spots could be remnants of the lateral mesoderm forming the

hindlimbs (Fig. 1H), suggesting that the mechanisms that specify them were activated in these embryos, but their outgrowth was impaired upon sustained stabilization of β-catenin in mesodermal derivatives. The low expression level of *Tbx4* in both domains may indicate that, unlike the paraxial mesoderm, formation of lateral mesoderm was strongly compromised in these embryos. Accordingly, expression of the splanchnic lateral mesoderm marker *Wnt2* was also strongly reduced in these embryos, being restricted to thin stripes ventral to the large mass of PSM (Fig. 1I,J).

These results show that persistent activation of β-catenin in PS derivatives does not induce neural differentiation, suggesting that the production of ectopic neural tubes in the prospective PSM region of *Tbx6* mutant embryos (Chapman and Papaioannou, 1998; Takemoto et al., 2011) is either independent of *Wnt3a* expression or requires that Wnt3a activity interacts with additional factors that are missing in the presence of *Tbx6*. Our findings also indicate that stabilized β-catenin in *T-Cre::β-catenin*$^{del(ex3)/+}$ embryos had little effect on the functional characteristics of their axial progenitors, as they were able to keep producing neural tissue and undergo trunk to tail transition to generate a tail bud.

Over-expression of Wnt3a in the epiblast causes severe axial abnormalities

The absence of any detectable effect of activated β-catenin on neural tube development in *T-Cre::β-catenin*$^{del(ex3)/+}$ embryos was somewhat surprising considering that Wnt/β-catenin has been shown to influence neural development from N-M progenitors (Takemoto et al., 2011; Martin and Kimelman, 2012). This absent phenotype could derive from the lack of β-catenin$^{del(ex3)}$ expression in the bipotent N-M progenitors of these embryos. Consistent with this hypothesis, the activity of the enhancer used to generate the *T-Cre::β-catenin*$^{del(ex3)/+}$ embryos was essentially detected in the mesodermal compartments with just residual activity in the neural tube (Perantoni et al., 2008) (Fig. S1A). Therefore, to evaluate the effect of Wnt3a on the axial progenitors we generated transgenic embryos in which *Wnt3a* was expressed under the control of an enhancer of the

Cdx2 gene. This regulatory element has been shown to be active in the posterior epiblast that contains the progenitors for tissues posterior to the forelimb bud (Gaunt et al., 2005; Benahmed et al., 2008; Jurberg et al., 2013), including mesoderm and neuroectoderm (Fig. S1B) (*Cdx2P-Wnt3a* transgenics). More than half of the *Cdx2P-Wnt3a* transgenic embryos harvested between E9.5 and E10.5 (n=121) were strongly malformed. Morphologically, these embryos were grossly normal up to the forelimb bud, but posterior to this level they were much shorter than their wild type littermates (Fig. 2A-F). These malformations were clearly different from those observed in *T-Cre::β-catenin*$^{del(ex3)/+}$ embryos (Figs 1 and 2). In particular, *Cdx2P-Wnt3a* transgenics lacked a morphologically identifiable neural tube but contained other recognizable body structures, including lateral protrusions resembling hindlimb buds, as well as small and misshapen paired segmented elements resembling somites (Fig. 2B,C,E,F,H). They also failed to rotate, remaining dorsally bent and ventrally open (Fig. 2F). In addition, these embryos contained a spherical cellular mass at their caudal end that seemed to be contiguous to other inner embryonic tissues (Fig. 2E,H,I). This ectopic mass resembled a similar structure observed in *T-Cre::β-catenin*$^{del(ex3)/+}$ embryos (Fig. 1H,J) and contained a complex vascular plexus as revealed by the endothelial marker PECAM-1 (Fig. 2I). Globally, the morphological characteristics of *Cdx2P-Wnt3a* transgenic embryos suggested that, despite their strong overall malformations caudal to the forelimbs, they could still preserve a degree of normal patterning.

High levels of Wnt3a in the epiblast affect the production of axial progenitor derivatives

To further characterize the nature of the tissues posterior to the forelimb buds in *Cdx2P-Wnt3a* transgenic embryos, we performed an extensive analysis using molecular markers for different embryonic tissues. Expression of the neural primordial marker *Sox2* was strongly down-regulated posterior to the forelimbs (Figs 3A,B and S2C,C'), indicating that the contribution of neural tissue to this

region was severely compromised as previously inferred from the embryo's morphology. Further analysis revealed the presence of most mesodermal compartments in the affected region. The identity of the somite-like structures was confirmed by *Uncx4.1* and *Raldh2* expression (Fig. 3 C-F). In the most posterior somites, *Uncx4.1* was expressed in a striped pattern (Fig. 3D'), indicating a relative conservation of AP polarity in these small somites. However, this pattern was lost in more anterior somites within the malformed tissue (Fig. 3D), suggesting that AP polarity was not maintained in more mature somites. In the posterior part of the embryo, the somitic mesoderm surrounded a mass of tissue, which was strongly positive for *Wnt3a* (Fig. 2D,G,G'), but negative for markers of the paraxial mesoderm including *Brachyury* (*T*), *Tbx6*, *Msgn*, *Fgf8* or its target *Spry4* (Fig. 3G-P). Instead, expression of these markers was restricted to the most posterior region of the transgenic embryos, suggesting that only a subset of the *Wnt3a*-positive cells entered a paraxial mesodermal fate and generated PSM competent to produce somites at the posterior end of the embryo. The PSM of *Cdx2P-Wnt3a* transgenics appeared reduced in its AP length and wider than in wild type embryos, which is compatible with the smaller somite size observed in the transgenics (Fig. 3I-P). The compact morphology of the *Cdx2P-Wnt3a* transgenics hampered proper analysis of the segmentation clock in the PSM. However, the determination front marker *Mesp2* was expressed in single bilateral stripes in the *Cdx2P-Wnt3a* transgenics (Fig. 3S). Although the domain of *Mesp2* expression could be slightly more extended in its AP size, it resembled the pattern observed in wild type embryos (Fig. 3R).

Together, these results indicate that over-activation of Wnt3a signaling in the epiblast prevents bipotent N-M progenitors from taking a neural fate, which is consistent with the zebrafish tail bud experiments by Martin and Kimelman (2012). However, activation of *Wnt3a* did not result in a massive production of paraxial mesoderm from epiblast progenitors. Instead, it led to an accumulation of a folded epithelial tissue that kept a degree of *Gdf11* and *Cyp26a1* expression, two markers typically associated with the epiblast (Fig. 4). These data thus suggest that overproduction of *Wnt3a* in the epiblast mostly promoted

accumulation of epithelial tissue with molecular characteristics closer to the epiblast rather than to any of its derivatives. Despite this, *Cdx2P-Wnt3a* embryos preserved the ability to produce mesodermal tissues that kept a degree of functionality in somitogenesis. The characteristics of the PSM in the *Cdx2P-Wnt3a* embryos are somewhat paradoxical considering the expanded PSM and lack of segmentation observed in *T-Cre::β-catenin*$^{del(ex3)/+}$ embryos (Aulehla et al., 2008). Such discrepancies might indicate that the respective phenotypes derived from dissimilar effects of Wnt3a/β-catenin activity in the different cellular compartments. Alternatively, they may have resulted from the different strategies used to activate the Wnt3a/β-catenin pathway in *Cdx2P-Wnt3a* and *T-Cre::β-catenin*$^{del(ex3)/+}$ embryos.

Wnt3a expression in the PSM affects somite polarity

To investigate these hypotheses, we over-expressed *Wnt3a* in the PSM using an enhancer of the *Dll1* gene (Beckers et al, 2000) (*Dll1-Wnt3a* transgenics). In these transgenics *Wnt3a* expression was observed throughout the whole PSM length (Fig. 5B), extending into the first few somites and was clearly excluded from the neural tube (Fig. S1C). A proportion of *Dll1-Wnt3a* transgenic embryos (16 out of 61) showed recognizable abnormal phenotypes, which were always much milder than those observed in either *T-Cre::β-catenin*$^{del(ex3)/+}$ or *Cdx2P-Wnt3a* embryos (Fig. 5). Only morphologically affected *Dll1-Wnt3a* transgenics embryos were used for further analyses. At E10.5, these transgenics extended their AP axis further than any of the other two types of embryos and preserved many of the normal embryonic characteristics. *Dll1-Wnt3a* embryos had an identifiable neural tube with normal *Sox2* expression (Fig. S2D,D'). They also contained recognizable somites, although they were abnormal in shape (Fig. 5C-D'). Interestingly, in the somites of *Dll1-Wnt3a* embryos, *Uncx4.1* expression was not restricted to their posterior half but extended throughout the whole somite (Fig. 5C',D'). This indicates that either the somites of these transgenic embryos were globally posteriorized or that they lacked anterior somitic compartments.

Consistent with this observation, somites of *Dll1-Wnt3a* embryos were totally negative for the anterior compartment marker *Tbx18* (Fig. 5E,F).

To analyze the origin of this phenotype, we evaluated *Tbx6* and *Mesp2* expression, because of their known roles in both segmentation and generation of AP polarity within the somites (White et al., 2005; Oginuma et al., 2005). *Tbx6* expression in *Dll1-Wnt3a* transgenics was essentially restricted to the tail bud mesenchyme, but lacked the sharp anterior border typically observed in wild type embryos (Fig. 5G,H). Instead, the *Tbx6* domain appeared anteriorly extended, following the expanded *Wnt3a* expression in these transgenic embryos (Fig. 5A,B). Expression of *Mesp2* was also abnormal in *Dll1-Wnt3a* embryos (Fig. 5I,J). Unlike in wild type embryos, *Mesp2* was not expressed as a single stripe, but extended anteriorly into the somite-containing region of the paraxial mesoderm, apparently matching the expanded *Tbx6* expression domain. *Lfng* expression in the PSM of *Dll1-Wnt3a* transgenic embryos presented variable patterns similar to those observed in wild type embryos (Fig. 5K-L''). This suggests that cycling of the segmentation clock is maintained in these transgenic embryos, similar to what has been observed in *T-Cre::β-catenin*$^{del(ex3)/+}$ embryos (Aulehla et al., 2008). Interestingly, *Lfng* expression in *Dll1-Wnt3a* embryos did not include the extra bands observed in more anterior areas of *T-Cre::β-catenin*$^{del(ex3)/+}$ embryos (Aulehla et al., 2008). The above results indicate that sustained Wnt3a signaling throughout the PSM is still compatible with intersomitic border formation when stimulated using the natural ligand and that Wnt3a expression in the PSM must be properly controlled to produce somites with anterior and posterior compartments.

Conservation of trunk-associated tissues in Cdx2P-Wnt3a transgenics

We next examined the impact of high levels of *Wnt3a* in the epiblast on trunk-related tissues other than those derived from N-M progenitors. *Cdx2P-Wnt3a* transgenics contained derivatives of the node and the most anterior region of the primitive streak. In particular, expression of *Shh* and *T* revealed the presence of

axial mesoderm, although reduced in extension and apparently split in two longitudinal domains at both sides along the midline of these embryos (Figs 3H' and 6B). We also detected the presence of visceral endoderm as shown by *Foxa1* expression (Fig. 6C,D). The very different patterns obtained for this gene when compared to wild type embryos most likely reflect the lack of ventral closure in the transgenics. Interestingly, we observed a strong domain of *Shh* expression at the level of the hindlimb buds (Fig. 6B), roughly corresponding to the most posterior limit of *Foxa1* expression (Fig. 6D). The position of this *Shh* expression domain potentially identifies the endodermal component of the developing cloaca (Perriton et al., 2002). Although the strong malformations observed in *Cdx2P-Wnt3a* transgenic embryos did not allow us to rule out that this domain represents an accumulation of axial mesoderm, the absence of an equivalent concentration of transcripts for *T* (Fig. 3H) seems to argue against this possibility. If the caudal domain of *Shh* expression indeed corresponds to the cloaca, it would indicate the existence of a degree of AP patterning in the visceral endoderm of *Cdx2P-Wnt3a* transgenics.

Morphological examination of *Cdx2P-Wnt3a* transgenics had suggested that, despite their strong malformations, these embryos contained forelimb and hindlimb buds (Fig. 2F). We confirmed their presence by expression of several markers, including *Fgf8*, *Spry4*, *Tbx4*, *Tbx5* and *Hand2* (Figs 3M-P and 6E-J). The restricted expression of *Tbx5* and *Tbx4* to the forelimb and hindlimb buds, respectively (Fig. 6E-H), indicated conservation of at least some regional specific characteristics along the AP axis of the severely malformed *Cdx2P-Wnt3a* embryos. In addition to the limb buds, *Cdx2P-Wnt3a* transgenics also contained other components of the lateral mesoderm, as shown by the expression of *Hand2* and *Wnt2* (Fig. 6I,L). Moreover, *Isl1* expression in the posterior part of *Cdx2P-Wnt3a* transgenics (Fig. 6M,N) and the extended *Tbx4* expression into ventral tissues between the hindlimb buds (Fig. 6F) suggest the presence of ventral lateral mesoderm. This mesodermal compartment is involved in the development of cloacal structures, thus supporting the interpretation that the *Shh*-positive domain in this area represents the endodermal component of the

cloaca. Interestingly, the ectopic spherical tissue mass at the caudal end of *Cdx2P-Wnt3a* transgenic embryos was positive for *Wnt2* and *Tbx4* (Fig. 6F,L). Expression of these two genes, together with the presence of a vascular plexus (Fig. 2I), suggests that this tissue corresponds to an ectopic outgrowth of lateral mesoderm. A similar *Wnt2* and *Tbx4*-positive mass was also observed in *T-Cre::β-catenin*$^{del(ex3)/+}$ embryos (Fig. 1H,J), suggesting that the apparent reduction of lateral mesoderm in these embryos derived from their abnormal specification upon stabilization of *β*-catenin in mesodermal derivatives. Finally, the presence of intermediate mesoderm in *Cdx2P-Wnt3a* transgenics was evidenced by the expression of *Raldh2* and *Pax2* in stripes lateral to the somites, resembling their position in wild type embryos (Figs 3E,F' and 6O,P). Altogether, these findings indicate that the tissues posterior to the forelimb buds of *Cdx2P-Wnt3a* embryos still preserved a surprisingly high degree of normal embryonic patterning despite the global severe malformation of the caudal region.

Posterior Hox gene expression is fairly conserved in Cdx2P-Wnt3a embryos

To further explore axial patterning in *Cdx2P-Wnt3a* embryos, we examined the expression of posterior Hox genes. Detailed analysis of the patterns produced by *Hoxa9*, *Hoxc10* and *Hoxd11* in *Cdx2P-Wnt3a* transgenics revealed that they mimicked several of the expression characteristics observed for those genes in wild type embryos (Fig. 7). For instance, *Cdx2P-Wnt3a* transgenics exhibited fairly well defined anterior Hox expression boundaries, progressively localized at more posterior levels, following the normal *Hoxa9-Hoxc10-Hoxd11* sequence (Fig. 7). In addition, the anterior expression boundaries for these genes also respected their relative wild type position when limb buds were taken as references. In particular, *Hoxa9* expression was first detected posterior to the forelimb bud (Fig. 7A,B), whereas the anterior *Hoxc10* and *Hoxd11* expression boundaries were localized at two different positions adjacent to the hindlimbs (Fig. 7C-F). Expression of these Hox genes in the lateral mesoderm of *Cdx2P-Wnt3a* transgenics was also similar to what was observed in wild type embryos.

Hence, *Hoxa9* expression was detected in the forelimb, in the hindlimb and in the interlimb lateral mesoderm, *Hoxd11* transcripts were observed in both anterior and posterior limb buds and *Hoxc10* expression was restricted to the hindlimb (Fig. 7). Together, these observations indicate that despite the strong morphological alterations that characterize *Cdx2P-Wnt3a* transgenics, Hox gene expression preserved many of its normal characteristics, including their collinear activation (Kmita and Duboule, 2003) and their appropriate correlation with specific morphological landmarks. However, the patterns obtained for these Hox genes in *Cdx2P-Wnt3a* embryos are congruent with an anteriorized position of their anterior expression boundaries when compared with wild type controls. This suggests the possibility that the compacted body morphology of *Cdx2P-Wnt3a* embryos resulted from a global posteriorization of the embryo caudal to the forelimb bud. It should be noted, however, that this phenotype might just be an indirect consequence of the strong alterations in the tissues more relevant to AP axis extension (neural tube and paraxial mesoderm) observed in *Cdx2P-Wnt3a* transgenic embryos. For instance, even if “normal patterns” (like Hox gene activation) are properly activated in tissues derived from N-M progenitors, if they fail to unfold properly along the AP axis they could become trapped within a folded epithelium and give a false impression of posteriorization.

Discussion

Wnt3a/β-catenin signaling has been shown to be essential at different stages during vertebrate axial growth. It has been reported that this signaling pathway modulates the fate of N-M progenitors (Takemoto et al., 2006; 2011; Martin and Kimelman, 2012; Nowotschin et al., 2012). Our data are consistent with this view and support the interpretation that, in mouse embryos, Wnt3a activity prevents these bipotent N-M progenitors from taking a neural fate, as high Wnt3a levels in the epiblast down-regulated *Sox2* expression. This is in agreement with previous studies in zebrafish embryos (Martin and Kimelman, 2012). It is also consistent with the *Wnt3a* mutant phenotype in the mouse, as mutant embryos contain neural tissue replacing mesodermal structures posterior to their forelimb buds

(Takada et al., 1994; Yoshikawa et al., 1997). However, they seem at odds with other reports suggesting that Wnt3a promotes *Sox2* expression in the precursors within the epiblast and that this expression has to be down regulated to produce mesodermal tissues (Takemoto et al., 2011; Nowotschin et al., 2012). A rationale for these apparent discrepancies is provided by a recent study (Tsakiridis et al., 2014) showing that different levels of Wnt signaling produce distinct effects on epiblast stem cells (EpiSCs). Low levels seemed to promote an uncommitted state, associated with expression of the main pluripotency markers, including *Sox2*. Grafting these cells into the epiblast of mouse embryos confirmed their multipotency, as they contributed to all epiblast derivatives. However, increasing Wnt levels in EpiSCs changed their properties so that when grafted into the mouse epiblast they were excluded from the neural tube and contributed only to mesodermal structures, indicating that high Wnt levels in these cells are incompatible with neural development. Therefore, we postulate that Wnt-dependent activation of *Sox2* in the epiblast may be related to the pluripotency role of this gene and not to its function in neural development. According to this view, activation of the neural pathway would require a Wnt-negative context in which *Sox2* (possibly activated through an alternative, Wnt-independent mechanism) would acquire a neural promoting function. This interpretation is consistent with fate maps of the epiblast (Tam and Behringer, 1997), showing that neural production occurs from regions adjacent to the most anterior part of the PS, which are exposed to low Wnt3a levels (Yoshikawa et al., 1997). It is also consistent with the activation of *Sox2* in *Wnt3a* mutants, which results in extra neural tissue (Nowotschin et al., 2012; Yoshikawa et al., 1997).

Interestingly, the reduction in neural tissue observed in *Cdx2P-Wnt3a* transgenics was not associated with a concomitant increase of mesodermal differentiation. *Cdx2P-Wnt3a* embryos seemed to contain all mesodermal compartments, indicating that high *Wnt3a* levels in the epiblast are compatible with mesoderm production. However, mesodermal markers were not observed in the folded epithelial sheet of *Cdx2P-Wnt3a* embryos, but only in tissues most likely produced upon delamination from that sheet. Such phenotype seems to

follow the natural pattern observed in the late gastrulating mouse embryo. In particular, *Wnt3a* expression is detected throughout most of the epiblast (Yoshikawa et al., 1997), whereas genes involved in paraxial mesoderm formation, like *Tbx6* (Chapman and Papaioannou, 1998; Chapman et al., 2003), are activated only after cells have left the epithelial compartment, despite their dependence on *Wnt3a* (Dunty et al., 2008; Takemoto et al., 2011; Nowotschin et al., 2012). Therefore, Wnt3a activity in the epiblast is necessary but not sufficient for mesodermal induction and might require concerted input of additional signals, which are very likely connected to the activity of the PS (Alev et al., 2013).

Considering all these observations, we propose that *Wnt3a* activity in the epiblast regulates the balance of progenitors taking a specific differentiation route or remaining multipotent, thus ensuring both constant production of new embryonic tissues and maintenance of a progenitor pool during axial growth (Fig. 8). These cell pools would be distributed along the AP axis of the epiblast, correlating with different *Wnt3a* expression levels observed in this tissue (Yoshikawa et al., 1997). The self-renewing axial progenitors would be confined to an area of moderate *Wnt3a* expression. In more anterior regions, cells exposed to Wnt signaling levels below a particular threshold would leave the uncommitted pool and activate the neural differentiation program. In more posterior areas, progenitors exposed to higher Wnt3a levels would also leave the self-renewing pool to acquire competence for mesodermal differentiation, which will only be activated upon interaction with the PS. In the embryo, the interaction of these cells with the PS is finely coordinated in a medial to lateral sequence relative to the PS (Tam and Behringer, 1997). Interestingly, this balance of cell compartments resembles that recently proposed for cultured EpiSCs (Tsakiridis et al., 2014). In *Cdx2P-Wnt3a* embryos, elevated Wnt stimulation disturbs such equilibrium, bringing most epiblast cells into the pool competent to mesodermal differentiation at the expense of the other two cell compartments. As a consequence, embryos fail to form neural tissues and become truncated due to a reduced self-renewing pool. In addition, the cell dynamics coordinating epiblast ingression through the PS would not be able to accommodate the increase of

mesoderm-competent cells, thus producing a remnant of cells that fail to delaminate and accumulate in an ill defined epithelial state that still preserves some epiblast characteristics.

It has been reported that activation of Wnt signaling in axial progenitors is enough to promote mesodermal differentiation (Martin and Kimelman, 2012). The apparent discrepancy between these observations and ours in *Cdx2P-Wnt3a* embryos might have resulted from the dissimilar experimental approaches used in both studies. Martin and Kimelman (2012) grafted progenitors containing a conditional activated form of β-catenin into the tail of recipient zebrafish embryos and followed the fate of the grafted cells. In contrast to our approach, activated Wnt signaling was restricted to cells inserted within an otherwise normal tail bud and, therefore, did not lead to major changes in the tissue structure of the recipient embryo. Under these conditions, the β-catenin positive cells could naturally become part of those excluded from a neural fate and enter the mesodermal compartment. This situation would be rather similar to the grafts of Wnt-activated EpiSCs into a normal recipient epiblast, which became incorporated into the embryonic mesodermal compartments (Tsakiridis et al., 2014), but divergent from ours, in which the whole epiblast was exposed to the increased Wnt3a signal.

Wnt/β-catenin during somitogenesis

An important component of this work is the observation that the patterns of cell response to Wnt/β-catenin activity change drastically as cells move from the epiblast into the paraxial mesoderm. This conclusion can be illustrated by the ability of Wnt/β-catenin signaling to promote *Tbx6* expression when activated in the PSM, which contrasts with the effects of *Wnt3a* over-expression in the epiblast, where *Tbx6* upregulation did not occur. Such change in tissue competence might be required to accommodate Wnt/β-catenin signaling to its role during somitogenesis (Aulehla et al., 2008; Dunty et al., 2008; Aulehla and Pourquié, 2010). In particular, Wnt/β-catenin blocks the segmentation program in

the PSM, as forced expression of a constitutively active form of β-catenin in the PSM prevents segmentation (Aulehla et al., 2008; Dunty et al., 2008). Thus, formation of a new intersomitic boundary requires that activity levels of this signaling fall below a threshold level, which results from the gradual decay in Wnt/β-catenin activity as cells occupy more anterior positions within the PSM (Aulehla et al., 2008). We now show that extended Wnt/β-catenin activity throughout the PSM is compatible with segmentation if Wnt3a is used to activate the pathway. The main difference between this strategy and those using β-catenin$^{del(ex3)}$ is that it preserves all associated feedback regulatory mechanisms (MacDonald et al., 2009), which are inoperative when using the inactivation-resistant β-catenin$^{del(ex3)}$ molecule. This might have functional consequences, most particularly when FGF signaling activity, which is also required for proper block of segmentation (Naiche et al., 2011), is also taken into account. Similar to Wnt signaling, FGF activity is not uniform throughout the PSM but forms a posterior to anterior gradient (Dubrulle and Pourquié, 2004), reaching non-functional levels in the anterior PSM. Under these conditions, feedback mechanisms might produce in the anterior PSM of *Dll1-Wnt3a* embryos transient decreases in the effective Wnt/β-catenin activity that, in the absence of FGFs, are enough to create a temporal window in which the segmentation program is not effectively blocked, eventually producing a new intersomitic border. Interestingly, although extended Wnt3a expression in the PSM allowed somitogenesis, the resulting somites lacked anterior compartments, indicating that proper control of Wnt/β-catenin signaling is also required to produce somites with normal AP polarity, although the role that Wnt signals play in this process remains to be clarified.

It has been recently shown that in zebrafish the anterior boundary of Wnt/β-catenin activity in the PSM does not coincide with the determination front, but is located in a more posterior position, midway through the AP length of the PSM (Bajard et al., 2014). These authors suggest that the segmentation program is already determined in the PSM when cells are no longer exposed to Wnt activity, but remains silent until these cells reach the anterior PSM, where the

segmentation program is executed. Similar to zebrafish, in mouse embryos nuclear β-catenin seems to be absent from the anterior half of the PSM (Aulehla et al., 2008), suggesting that this mechanism might not be a zebrafish peculiarity. In addition, considering the phenotype of *Dll1-Wnt3a* transgenic embryos it will be interesting to determine whether somites acquire their AP polarity already when Wnt/β-catenin activity falls below a threshold level in the posterior PSM and only implemented later when the new segment is formed. Supporting this possibility, expression of *Mesp2* and *Tbx6*, which are involved in both segmentation and AP patterning of the somites (Oginuma et al., 2005; White et al., 2005), was anteriorly extended in *Dll1-Wnt3a* transgenics, mirroring the more anteriorly positioned and disorganized border of *Wnt3a* expression observed in these embryos.

In summary, together with the results of previous studies, our data indicate sequential roles for *Wnt3a* in different processes involved in axial extension of the vertebrate embryo. Proper coordination of these processes depends on specific patterns of activation and repression of the Wnt/β-catenin pathway, in conjunction with a progressive change in cell competence to respond to such signals. The mechanisms controlling cell competence during axial extension remain to be further elucidated.

Acknowledgements

We are grateful to Alexander Aulehla for providing us with *T-Cre::β-catenin*$^{del(ex3)/+}$ embryos, obtained in the context of his collaboration with Mark Lewandoski and Makoto Taketo. We would like to thank José Belo, Jacqueline Deschamps, Denis Duboule, Achim Gossler, Bernhard Herrmann, Andreas Kispert, Malcolm Logan, Andrew McMahon and Erik Olson for sending plasmids containing cDNAs, regulatory elements and probes for *in situ* hybridization. This work was supported by grants PTDC/BIA-BCM/110638/2009 and PTDC/SAU-BID/110640/2009 to M.M. and by PhD fellowships SFRH/BD/33562/2008 to A.D.J. and SFRH/BD/51876/2012 to R.A.

References

Alev, C., Wu, Y., Nakaya, Y., Sheng, G. 2013. Decoupling of amniote gastrulation and streak formation reveals a morphometric unity in vertebrate mesoderm induction. Development 140, 2691-2696.

Aulehla, A., Wiegraebe, W., Baubet. V., Wahl, M. B., Deng, C., Taketo, M., Lewandoski, M., Pourquié, O. 2008. A beta-catenin gradient links the clock and wavefront systems in mouse embryo segmentation. Nature Cell. Biol. 10, 186-193.

Aulehla, A., Pourquié, O. 2010. Signaling gradients during paraxial mesoderm development. Cold Spring Harb. Perspect. Biol. 2, a000869.

Bajard, L., Morelli, L. G., Ares, S., Pécréaux, J., Jülicher, F., Oates, A. C. 2014. Wnt-regulated dynamics of positional information in zebrafish somitogenesis. Development 141, 1381-1391.

Beckers, J., Caron, A., Hrabe de Angelis, M., Hans, S., Campos-Ortega, J. A., Gossler, A. 2000. Distinct regulatory elements direct delta1 expression in the nervous system and paraxial mesoderm of transgenic mice. Mech. Dev. 95, 23-34.

Benahmed, F., Gross, I., Gaunt, S. J., Beck, F., Jehan, F., et al. 2008. Multiple regulatory regions control the complex expression pattern of the mouse Cdx2 homeobox gene. Gastroenterology 135, 1238-1247.

Cambray, N., Wilson, V. 2002. Axial progenitors with extensive potency are localised to the mouse chordoneural hinge. Development 129, 4855-4866.

Cambray, N., Wilson, V. 2007. Two distinct sources for a population of maturing axial progenitors. Development 134, 2829-2840.

Carlson, B. M. 1999. Human embryology and developmental biology, Second Edition (Mosby, Inc. St. Louis).

Carvajal, J.J., Cox, D., Summerbell, D., Rigby, P.W. 2001. A BAC transgenic analysis of the Myf4/Myf5 locus reveals interdigitated elements that control activation and maintenance of gene expression during muscle development. Development 128, 1857-1868.

Chapman, D. L., Papaioannou, V. E. 1998. Three neural tubes in mouse

embryos with mutations in the T-box gene Tbx6. Nature 391, 695-697.

Chapman, D. L., Cooper-Morgan, A., Harrelson, Z., Papaioannou, V. E. 2003. Critical role for Tbx6 in mesoderm specification in the mouse embryo. Mech. Dev. 120, 837-847.

Dubrulle, J., Pourquié, O. 2004. Fgf8 mRNA decay establishes a gradient that couples axial elongation to patterning in the vertebrate embryo. Nature 427, 419-422.

Dunty, W. C., Biris, K. K., Chalamalasetty, R. B., Taketo, M. M., Lewandoski, M., Yamaguchi, T. P. 2008. Wnt3a/beta-catenin signaling controls posterior body development by coordinating mesoderm formation and segmentation. Development 135, 85–94.

Gaunt, S. J., Drage, D., Trubshaw, R. C. 2005. cdx4/lacZ and cdx2/lacZ protein gradients formed by decay during gastrulation in the mouse. Int. J. Dev. Biol. 49, 901-908.

Harada, N., Tamai, Y., Ishikawa, T., Sauer, B., Takaku, K., et al. 1999. Intestinal polyposis in mice with a dominant stable mutation of the beta-catenin gene. EMBO J. 18, 5931-5942.

Hayashi, S., McMahon, A. P. 2002. Efficient recombination in diverse tissues by a tamoxifen-inducible form of Cre: tool for temporally regulated gene activation/inactivation in the mouse. Dev. Biol. 244, 305-318.

Jurberg, A. D., Aires, R., Varela-Lasheras, I., Nóvoa, A., Mallo, M. 2013. Switching axial progenitors from producing trunk to tail tissues in vertebrate embryos. Dev. Cell 25, 451-462.

Kanzler, B., Kuschert, S. J., Liu, Y. H., Mallo, M. 1998. Hoxa-2 restricts the chondrogenic domain and inhibits bone formation during development of the branchial area. Development 125, 2587-2597.

Kmita, M., Duboule, D. 2003. Organizing axes in time and space; 25 years of colinear tinkering. Science 301, 331-333.

Martin, B. L., Kimelman, D. 2012. Canonical Wnt signaling dynamically controls multiple stem cell fate decisions during vertebrate body formation. Dev. Cell 22, 223-232.

MacDonald, B.T., Tamai, K., He, X. 2009. Wnt/beta-catenin signaling: components, mechanisms, and diseases. Dev Cell. 17, 9-26.

Naiche, L.A., Holder, N., Lewandoski, M. 2011. FGF4 and FGF8 comprise the wavefront activity that controls somitogenesis. Proc. Natl. Acad. Sci. U S A. 108, 4018-4023.

Nowotschin, S., Ferrer-Vaquer, A., Concepcion, D., Papaioannou, V. E., Hadjantonakis, A. K. 2012. Interaction of Wnt3a, Msgn1 and Tbx6 in neural versus paraxial mesoderm lineage commitment and paraxial mesoderm differentiation in the mouse embryo. Dev. Biol. 367, 1-14.

Oginuma, M., Niwa, Y., Chapman, D. L., Saga, Y. 2008. Mesp2 and Tbx6 cooperatively create periodic patterns coupled with the clock machinery during mouse somitogenesis. Development 135, 2555-2562.

Perantoni, A. O., Timofeeva, O., Naillat, F., Richman, C., Pajni-Underwood, S., et al. 2005. Inactivation of FGF8 in early mesoderm reveals an essential role in kidney development. Development 132, 3859-3871.

Perriton, C. L., Powles, N., Chiang, C., Maconochie, M. K., Cohn, M. J. 2002. Sonic hedgehog signaling from the urethral epithelium controls external genital development. Dev. Biol. 247, 26-46.

Soriano, P. 1999. Generalized lacZ expression with the ROSA26 Cre reporter strain. Nat. Genet 21, 70-71.

Stern, C. D., Charité, J., Deschamps, J., Duboule, D., Durston, A. J., et al. 2006. Head-tail patterning of the vertebrate embryo: one, two or many unresolved problems? Int. J. Dev. Biol. 50, 3-15.

Takada, S., Stark, K. L., Shea. M. J., Vassileva, G., McMahon, J. A., McMahon, A. P. 1994. Wnt-3a regulates somite and tailbud formation in the mouse embryo. Genes Dev. 8, 174-189.

Takemoto, T., Uchikawa, M., Kamachi, Y., Kondoh, H. 2006. Convergence of Wnt and FGF signals in the genesis of posterior neural plate through activation of the Sox2 enhancer N-1. Development 133, 297-306.

Takemoto, T., Uchikawa, M., Yoshida, M., Bell, D. M., Lovell-Badge, R., et al. 2011. Tbx6-dependent Sox2 regulation determines neural or mesodermal fate in axial stem cells. Nature 470, 394-398.

Tam, P. P., Behringer, R. R. 1997. Mouse gastrulation: the formation of a mammalian body plan. Mech. Dev. 68, 3-25.

Tsakiridis, A., Huang, Y., Blin, G., Skylaki, S., Wymeersch, F., et al. 2014. Distinct Wnt-driven primitive streak-like populations reflect in vivo lineage precursors. Development 141, 1209-1221.

Tzouanacou, E., Wegener, A., Wymeersch, F. J., Wilson, V., Nicolas, J.-F. 2009. Redefining the progression of lineage segregations during mammalian embryogenesis by clonal analysis. Dev. Cell 17, 365-376.

White, P. H., Farkas, D. R., Chapman, D. L. 2005. Regulation of Tbx6 expression by Notch signaling. Genesis 42, 61-70.

Wilson, V., Olivera-Martinez, I., Storey, K. G. 2009. Stem cells, signals and vertebrate body axis extension. Development 136, 2133-2133.

Yoshikawa, Y., Fujimori, T., McMahon, A. P., Takada, S. 1997. Evidence that absence of Wnt-3a signaling promotes neuralization instead of paraxial mesoderm development in the mouse. Dev. Biol. 183, 234-242.

FIGURE LEGENDS

Figure 1. Molecular patterning in *T-Cre::β-catenin*$^{del(ex3)/+}$ embryos. Wild type (A, C, E, G and I) and *T-Cre::β-catenin*$^{del(ex3)/+}$ mutant (B, D, F, H and J) embryos were analyzed at E10.5 by whole mount in situ hybridization. A, B. Expression of *Sox2*. The arrows indicate the neural tube; the ventral mass in the mutant embryos (arrowhead in B) is negative for *Sox2*. C, D. Expression of *Tbx6*. The ventral mass in the mutant embryos showed positive staining (arrowhead in D). E, F. Expression of *Hoxc10*. The anterior expression border in the neural tube (arrows) and in the ventral mass of the mutant embryos (arrowhead in F) are indicated. G, H. *Tbx4* expression marks the position of the cloaca (arrows) and of the hindlimbs in the wild type embryo (G) and several spots within the ventral mass of the mutant embryo (arrowheads in H). The asterisk indicates a *Tbx4*-positive ectopic tissue growth in the mutant embryos. I, J. Expression of *Wnt2* marks the lateral mesoderm (arrowheads). The asterisk indicates a *Wnt2*-positive ectopic tissue growth in the mutant embryos.

Figure 2. Effect of *Wnt3a* over-expression in the epiblast. A-C. Wild type embryos at E10.5 stained for *Wnt3a* (A) or with hydrochloric carmine for their external morphology (B, C). D. Dorsal view of *Wnt3a* expression in a *Cdx2P-Wnt3a* transgenic embryo. Section planes corresponding to the pictures shown in G and G' are indicated. E, F. Lateral and ventral views, respectively, of a *Cdx2P-Wnt3a* transgenic embryo stained by carmine. The asterisk indicates an ectopic mass observed in these embryos. The arrows indicate the limb buds. G, G'. Transversal sections of a *Wnt3a*-stained *Cdx2P-Wnt3a* transgenic embryo through the levels indicated in D. H. Detailed view of a *Cdx2P-Wnt3a* transgenic embryo to show the somites (arrowhead) just next to the hindlimb bud. The asterisk indicates an ectopic mass observed in these embryos. I. PECAM-1 staining of the ectopic mass labeled with an asterisk in E and H reveals a blood plexus. The image shows the projection of multiple virtual sections by confocal microscopy.

Figure 3. Molecular analysis of *Cdx2P-Wnt3a* transgenic embryos. Wild type (A, C, E, G, I, K, M, O and R) and *Cdx2P-Wnt3a* transgenic (B, D, D', F, F', H, H', J, L, N, P and S) embryos were analyzed for different molecular markers either at E9.5 (A,B,G-S) or at E10.5 (C-F'). A, B. Expression of *Sox2*. The arrow marks the position of the forelimb bud in the transgenics. C-D'. Expression of *Uncx4.1*. D' Close up of the caudal part of a transgenic embryo demonstrating a striped expression pattern in the somites (arrowheads). The asterisk marks the undifferentiated folded mass between the caudal somites. E-F'. Expression of *Raldh2* revealed caudal somites (arrowhead in F) and the intermediate mesoderm (arrow in F'). G-H'. Expression of *Brachyury* revealed the notochord (arrow) and the PSM (arrowhead); the asterisk marks the undifferentiated folded mass. H'. Ventral view of the posterior embryonic area showing a split notochord (arrow). I, J. Expression of *Tbx6* in the PSM (arrowheads). The asterisk marks the undifferentiated folded mass. K, L. Expression of *Msgn* in the PSM (arrowheads). The asterisk indicates the undifferentiated folded mass. M, N. Expression of *Fgf8* reveals the PSM (arrowheads) and the position of the limb buds (arrows). O, P. Expression of *Spry4* indicates the PSM (arrowheads) and the position of the limb buds (arrows). Expression of *Mesp2* marks the determination front in the anterior PSM (arrowheads).

Figure 4. Epiblast morphology of *Cdx2P-Wnt3a* transgenic embryos. A-B''. *Cyp26a1* expression in wild type embryos (A-A') at E9.0 and in the transgenics (B-B'') at E9.5. A'. Transversal section through the level indicated in A. Expression is mostly restricted to the epiblast (arrow). B' and B'' show sections through the areas indicated in B. Expression was observed in the epithelium of the posterior part of the embryo (arrows). C-D'. *Gdf11* expression in wild type embryos (C-C') at E9.5 and transgenics (D-D') at E10.5. C'. Tranversal section through the level indicated in C. Expression was observed in the epiblast (arrow) and in the dorsal part of the surface ectoderm of the posterior embryo. D'. Transversal section through the level indicated in D. Expression was observed in the folded epithelium at the posterior part of the embryo (arrows).

Figure 5. Molecular analysis of *Dll1-Wnt3a* transgenic embryos. Wild type (A, C, C' E, G, I and K-K'') and *Dll1-Wnt3a* transgenic (B, D, D', F, H, J and L-L'') embryos were analyzed for different molecular markers. A, B. Expression of *Wnt3a* in the tail tip of normal embryos (arrow) and an extended domain in the PSM of transgenic embryos (bracket). C-D'. Expression of *Uncx4.1* in the somites. C' and D' Close ups of the interlimb somites. C'. Restricted expression to posterior somite half in the wild type (contoured region) is not observed in the transgenics (D'). E, F. Expression of *Tbx18* is absent in the paraxial mesoderm of transgenic embryos (F), but it is still present in control regions such as the limb buds. G, H. Expression of *Tbx6*. The arrow indicates anterior expression border in the PSM of normal embryos (G) and the bracket marks an extended domain at the anterior PSM border of the transgenic embryo (H). I, J. Expression of *Mesp2* is restricted to a defined band in the anterior part of the PSM in normal embryos (I) and extended (bracket) in transgenic embryos (J). K-L''. Cycling expression of *Lfng* in the tails of three different wild type (K-K") and three different *Dll1-Wnt3a* transgenic embryos (L-L").

Figure 6. Molecular analysis of *Cdx2P-Wnt3a* transgenic embryos. Wild type (A, C, E, G, I, K, M and O) and *Cdx2P-Wnt3a* transgenic (B, D, F, H, J, L, N and P) embryos were analyzed for different molecular markers at E10.5 (A-L) or E9.5 (M-P). A, B. Expression of *Shh* marks the endodermal component of the cloaca (arrows) and the notochord (arrowheads). C, D. Expression of *Foxa1* indicates endodermal tissue (arrows). E, F. Expression of *Tbx4* marks the hindlimbs (arrows), the mesodermal component of the cloaca (arrowheads) and an ectopic vascular mass in the transgenics (asterisk). G, H. Expression of *Tbx5* marks the forelimbs (arrows). I, J. Expression of *Hand2* indicates the lateral mesoderm between the limb buds (arrows). K, L. Expression of *Wnt2* labels the lateral mesoderm between the limb buds (arrows) and the ectopic vascular mass (asterisk). M, N. Expression of *Isl1* labels the mesodermal component of the

cloaca (arrows). O, P. Expression of *Pax2* reveals intermediate mesoderm (arrows).

Figure 7. Hox gene expression in *Cdx2P-Wnt3a* transgenic embryos. A, B. *Hoxa9* expression in wild type (A) and *Cdx2P-Wnt3a* transgenic (B) embryos at E9.5. C, D. *Hoxc10* expression in wild type (C) and *Cdx2P-Wnt3a* transgenic (D) embryos at E10.5. E, F. *Hoxd11* expression in wild type (E) and *Cdx2P-Wnt3a* transgenic (F) embryos at E10.5. Black arrows show the hindlimb position, black arrowheads the position of the forelimb and the red arrows the anterior expression border in medial tissues.

Figure 8. A model for Wnt3a roles on axial progenitors in the epiblast. A. In wild type embryos, the levels of Wnt3a expression in the epiblast (represented by red color intensity) are lower next to the anterior part of the primitive streak than in more posterior areas. Progenitors exposed to moderate levels of Wnt activity are involved in keeping the progenitor pool required for further axial growth. Rostral to this area, progenitors exposed to lower levels of Wnt3a switch on a neural program and contribute to the growing neural tube. At more caudal levels, higher Wnt3a activity brings progenitors into a state competent to produce mesoderm. Upon interaction with the primitive streak, these cells delaminate from the epithelial layer to produce mesoderm. B. In *Cdx2P-Wnt3a* embryos, progenitors are all exposed to high Wnt3a levels, which bring them to the mesoderm-prone state. This fate is subsequently activated upon interaction with the primitive streak.

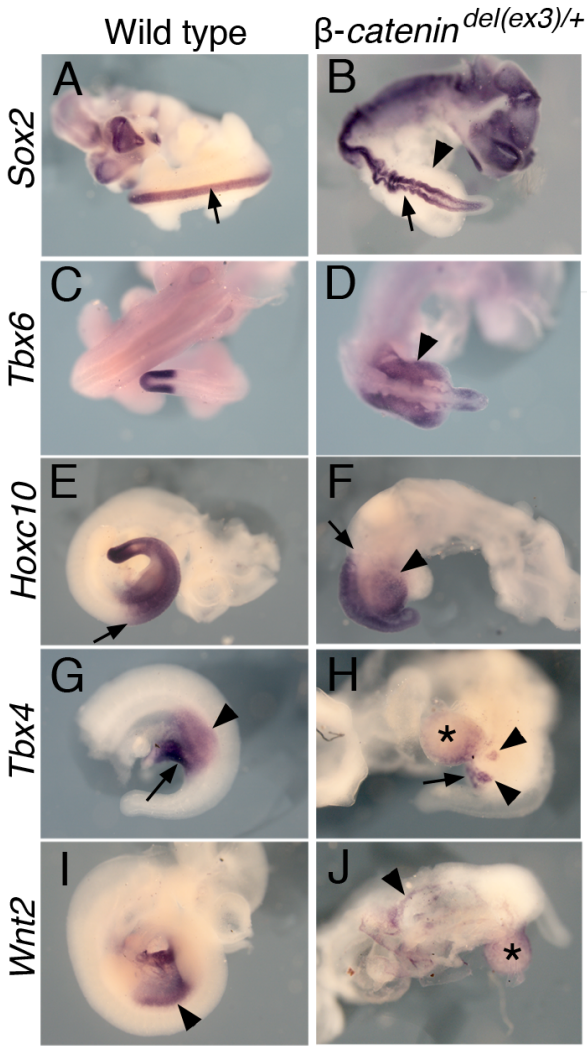
Wild type
β-catenin del(ex3)/+
Sox2
Tbx6
Hoxc10
Tbx4
Wnt2
A
B
C
D
E
F
G
H
I
J
*
*

Figure 1

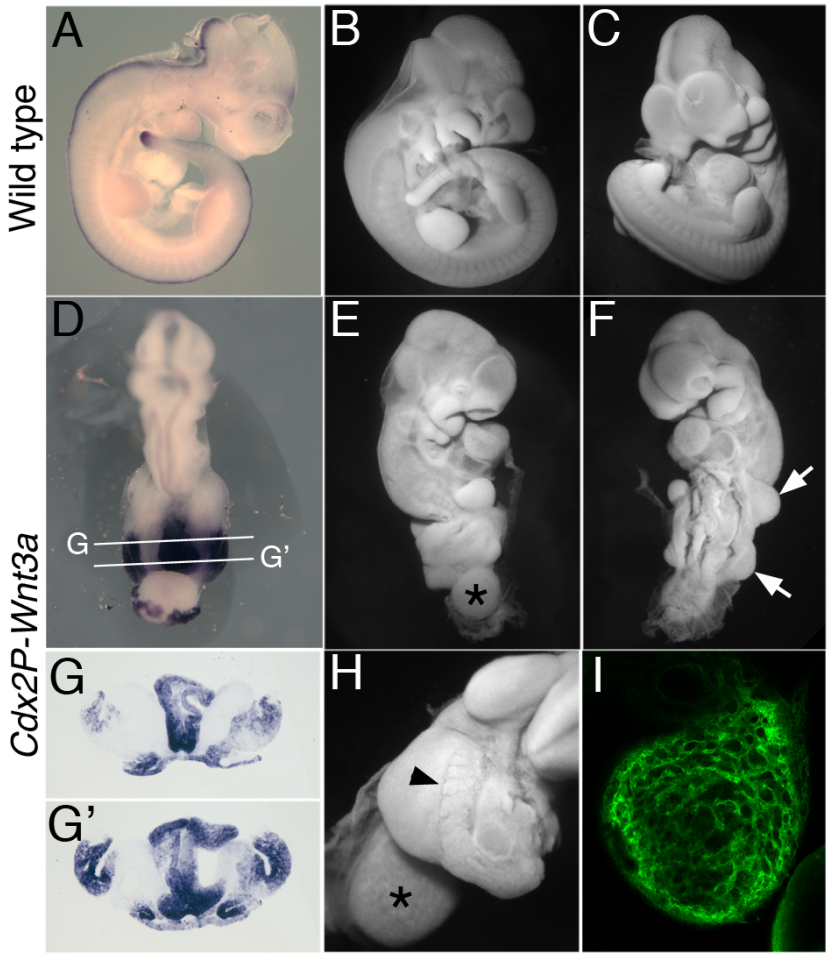

Figure 2

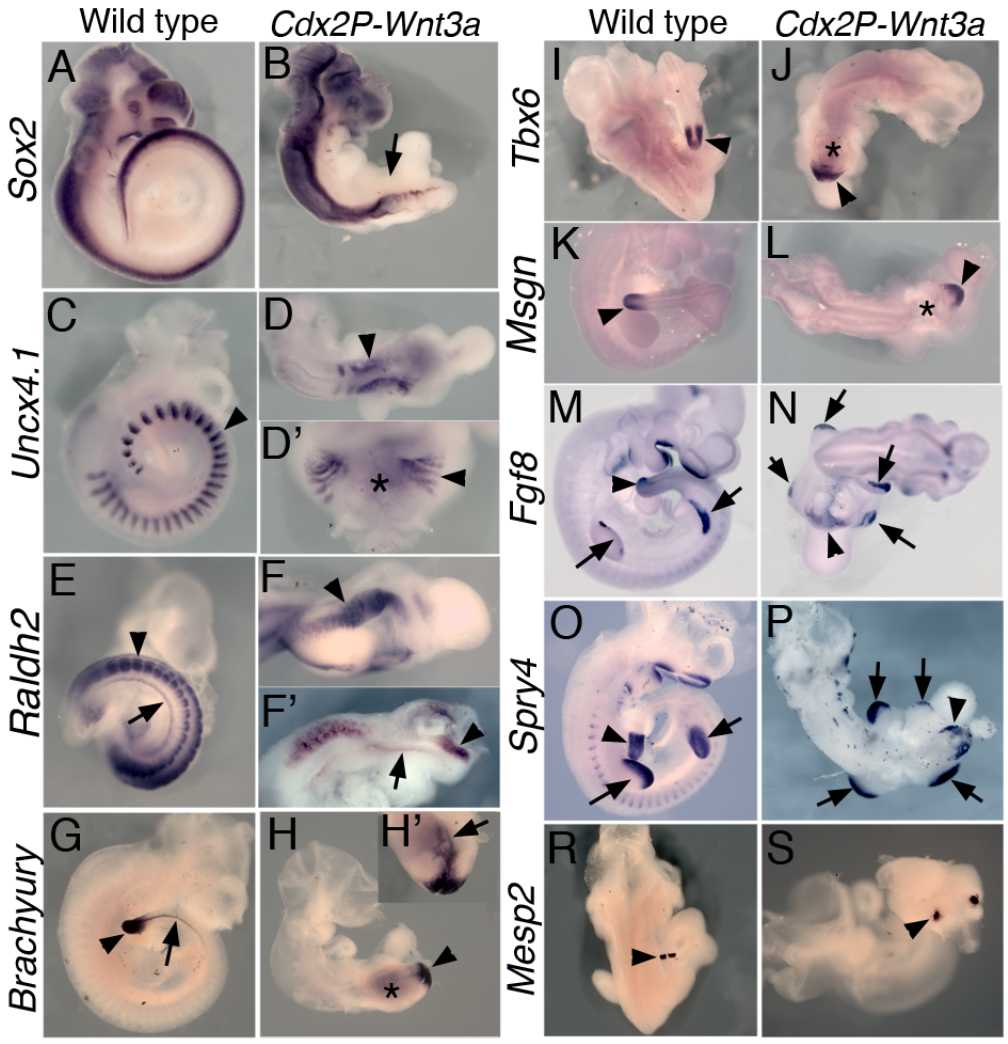
Wild type
Cdx2P-Wnt3a
Wild type
Cdx2P-Wnt3a
Sox2
Uncx4.1
Raldh2
Brachyury
Tbx6
Msgn
Fgf8
Spry4
Mesp2
A
B
C
D
D'
E
F
F'
G
H
H'
I
J
K
L
M
N
O
P
R
S

Figure 3

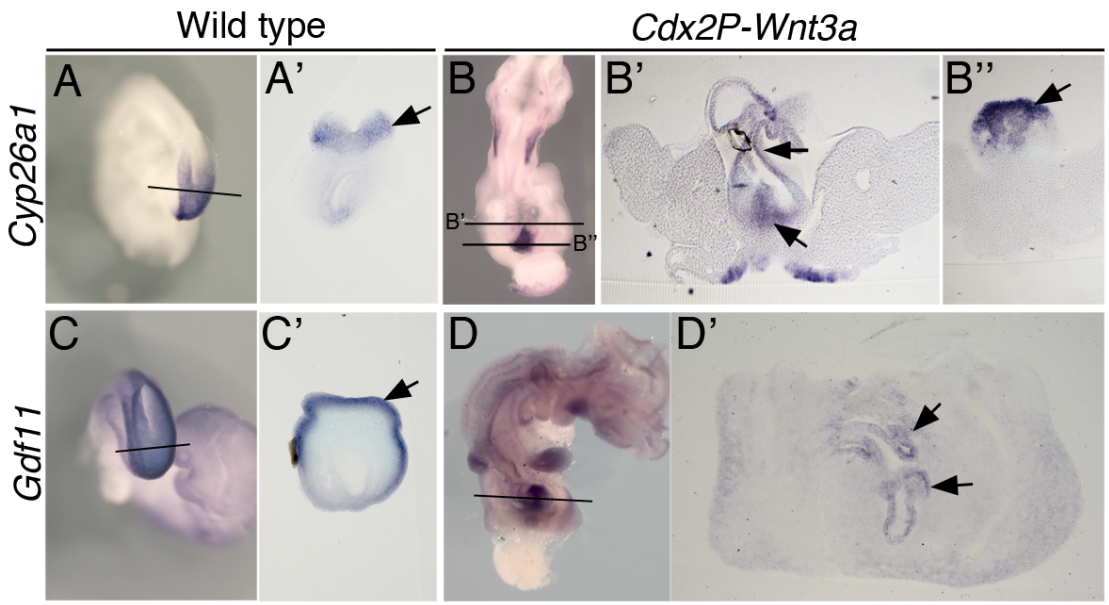

Figure 4

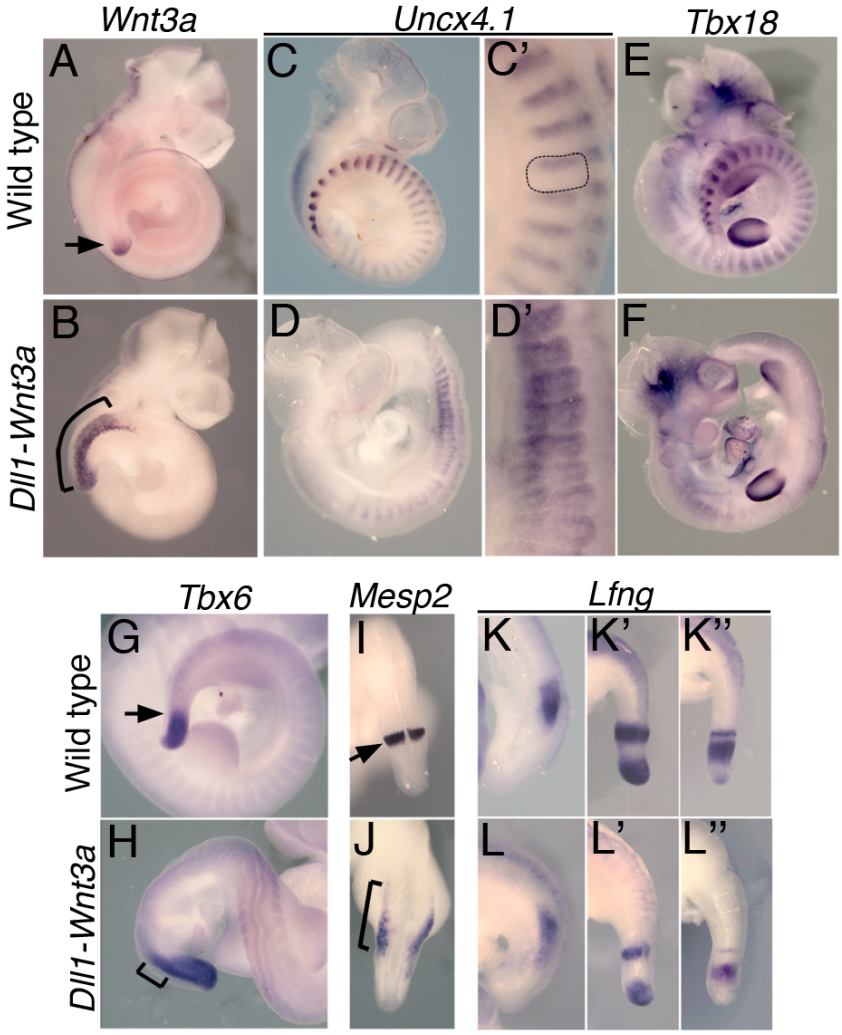
Wnt3a
Uncx4.1
Tbx18
Wild type
Dll1-Wnt3a
A
B
C
C'
D
D'
E
F
Tbx6
Mesp2
Lfng
Wild type
Dll1-Wnt3a
G
H
I
J
K
K'
K''
L
L'
L''

Figure 5

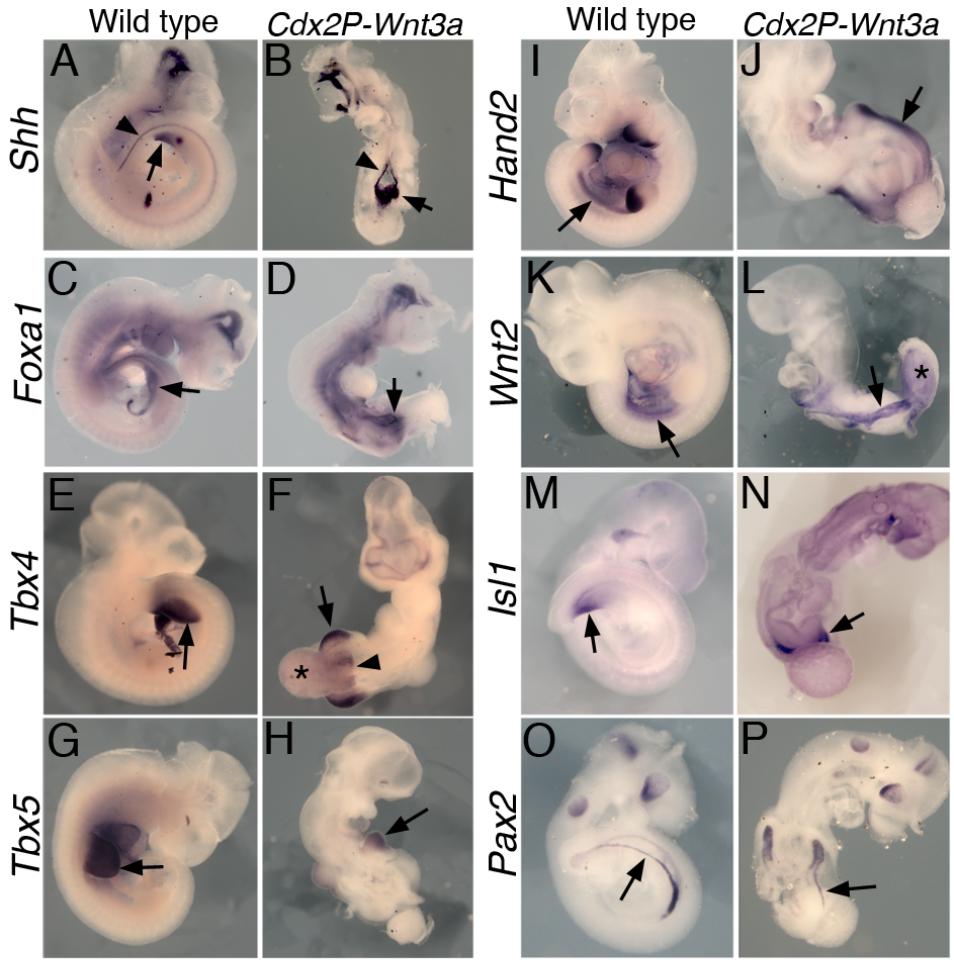
Wild type
Cdx2P-Wnt3a
Wild type
Cdx2P-Wnt3a
A
B
I
J
Shh
Hand2
C
D
K
L
Foxa1
Wnt2
E
F
M
N
Tbx4
Isl1
G
H
O
P
Tbx5
Pax2

Figure 6

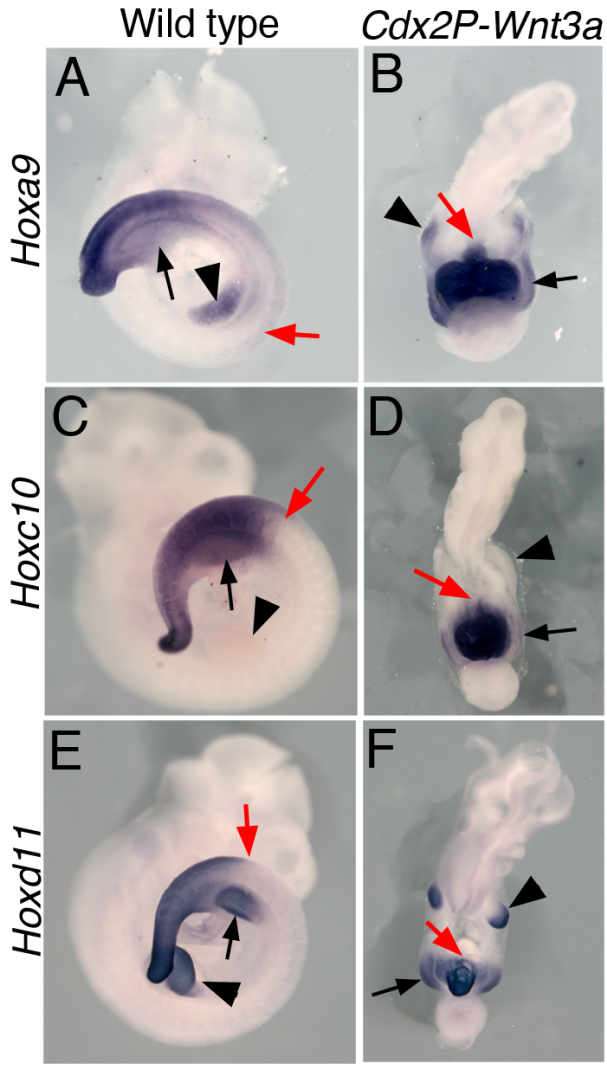

Figure 7

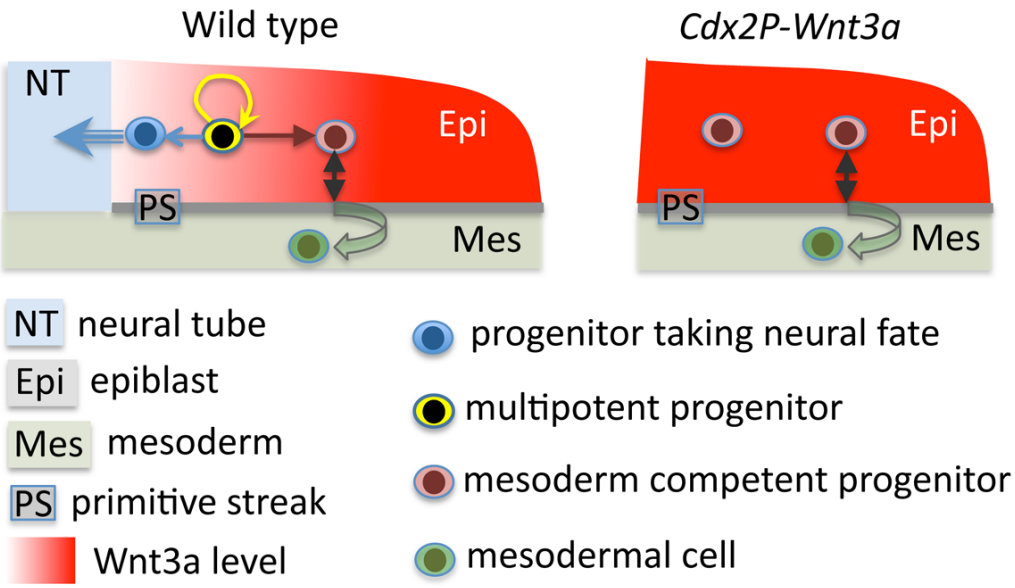
Wild type
Cdx2P-Wnt3a
NT
Epi
PS
Mes
Epi
PS
Mes
NT neural tube
Epi epiblast
Mes mesoderm
PS primitive streak
Wnt3a level
progenitor taking neural fate
multipotent progenitor
mesoderm competent progenitor
mesodermal cell

Figure 8

SUPPLEMENTARY FIGURES

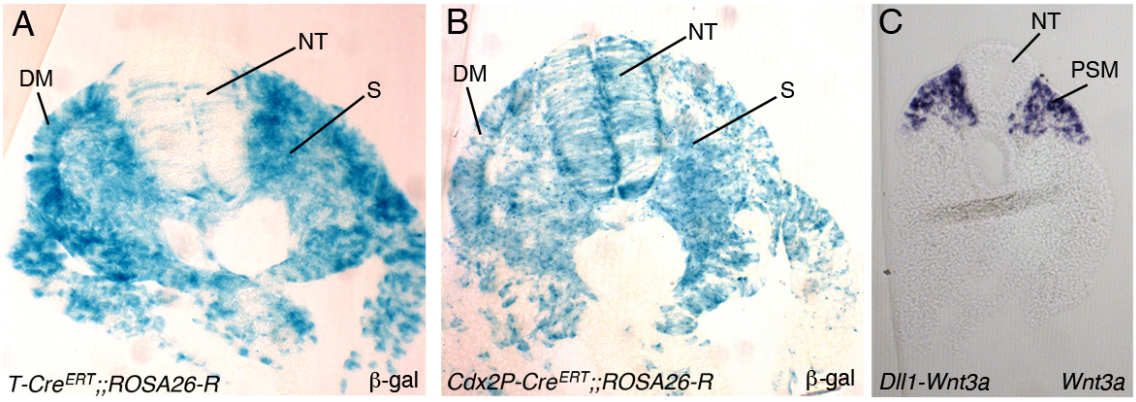

Figure S1. Tissue distribution of the *T*, *Cdx2P* and *Dll1* enhancer activity. A, B. The activity of the *T* (A) and the *Cdx2P* (B) enhancers was compared by analysis of β-galactosidase activity from the *ROSA26* reporter allele in embryos containing transgenes driving Cre^{ERT} expression under the control of one of the two enhancers (B). In both cases, Cre activity was stimulated by tamoxifen administration at E7.5 and E8.0 and the embryos were collected at E9.5. After staining for β-galactosidase, the embryos were sectioned using a vibratome. The pictures show transverse sections through equivalent areas of the embryos. In *T-*Cre^{ERT}*;;ROSA26-R* embryos the mesoderm was strongly labeled whereas the neural tube contained only a few labeled cells. In *Cdx2P-*Cre^{ERT}*;;ROSA26-R* embryos, both neural tube and mesodermal tissues were labeled similarly. C. Transverse sections through the caudal part of a *Dll1-Wnt3a* transgenic embryo (shown in Fig. 5B) revealed that *Wnt3a* expression was restricted to the presomitic mesoderm. DM: dermomyotome; NT: neural tube; PSM: presomitic mesoderm; S: sclerotome.

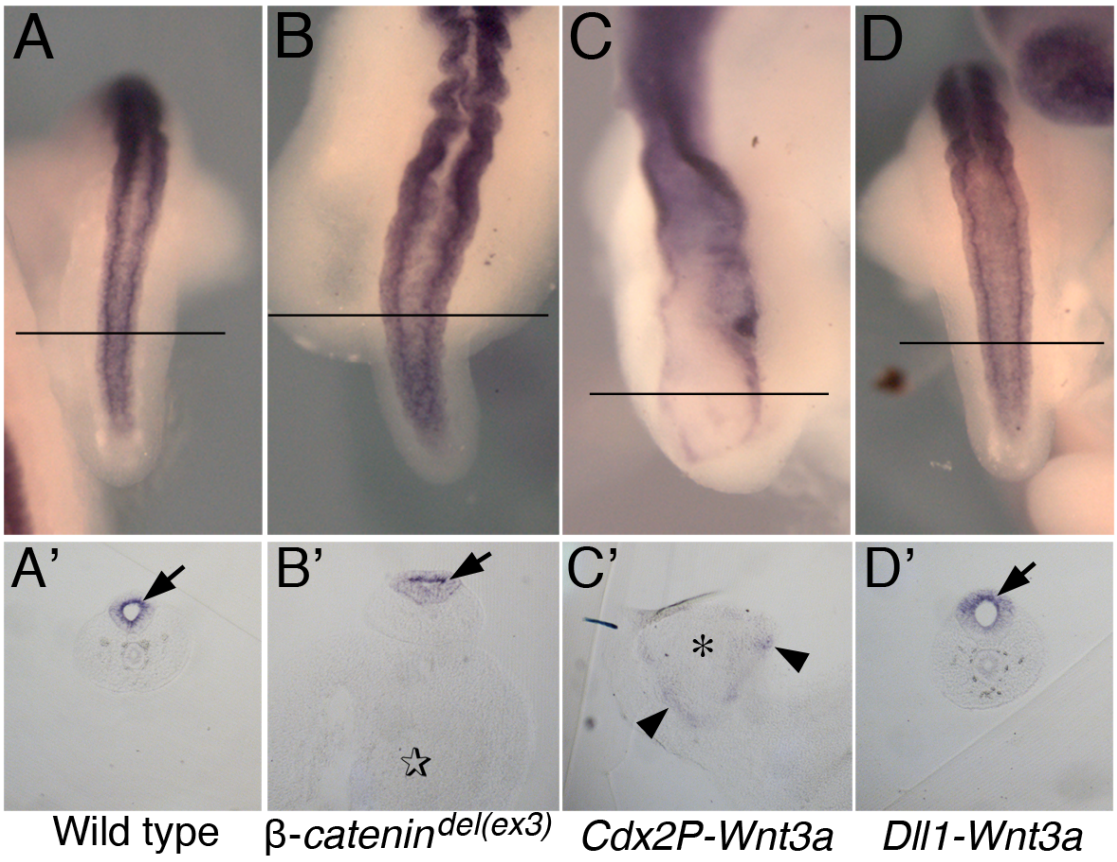

Figure S2. *Sox2* expression in the caudal region of different transgenic embryos. Close ups of the tail bud of wild type (A), a *T-Cre::β-catenin*$^{del(ex3)/+}$ (B), a *Cdx2P-Wnt3a* (C) and a *Dll1-Wnt3a* (D) E10.5 embryos stained for *Sox2* expression by whole mount in situ hybridization. A', B', C' and D' show transversal sections through the areas indicated in the corresponding embryo. The arrows indicate the neural tube. The arrowheads in C' indicate residual *Sox2* expression and the asterisk marks the position of the folded epithelium. The star in B' indicates the ventral mass observed in *T-Cre::β-catenin*$^{del(ex3)/+}$ embryos.